Robust linear dependence of thermal conductance on radial strain in carbon nanotubes

2012 New J. Phys. 14 013053

(http://iopscience.iop.org/1367-2630/14/1/013053)

New Journal of Physics
The open-access journal for physics

Robust linear dependence of thermal conductance on radial strain in carbon nanotubes

Hongqin Zhu, Yong Xu[1,2], Bing-Lin Gu and Wenhui Duan[1]
Department of Physics and State Key Laboratory of Low-Dimensional Quantum Physics, Tsinghua University, Beijing 100084, People's Republic of China
E-mail: dwh@phys.tsinghua.edu.cn and yongxu@fhi-berlin.mpg.de

New Journal of Physics **14** (2012) 013053 (10pp)
Received 21 September 2011
Published 25 January 2012
Online at http://www.njp.org/
doi:10.1088/1367-2630/14/1/013053

Abstract. Nanotubes have recently been experimentally demonstrated to be perfect phonon waveguides. To explore the underlying physics, we present atomic scale calculations of thermal transport in carbon nanotubes under radial strain using the nonequilibrium Green's function method. It is found that the thermal conductance exhibits a robust linear response behavior to radial strain over the whole elastic range. A detailed analysis of phonon transmission reveals that an elastic radial strain can be viewed as a perturbation of the transport of most of the low-frequency phonons. This is attributed to the unique bonding configuration of nanotubes, which can be well preserved even under severe deformation. Such a structural response to deformation, which is rare in other systems, explains the robust thermal transport in nanotubes against severe radial deformation.

[1] Authors to whom any correspondence should be addressed.
[2] Present address: Fritz-Haber-Institut der Max-Planck-Gesellschaft, Faradayweg 4-6, D-14195 Berlin, Germany.

Contents

1. Introduction

Carbon nanotubes (CNTs) possess unusually high thermal conductivity [1–4], desirable for heat dissipation. For instance, vertically aligned CNTs as thermal interface materials enhance thermal conductivity by almost two orders of magnitude [5], and aligned CNT arrays as cooling elements in chips show advantages over other materials [6]. It is well known that low-dimensional materials exhibit physical properties distinct from those of bulk materials owing to important quantum effects caused by confinement. Knowledge of the thermal transport in CNTs—typical quasi-one-dimensional (1D) systems—is also valuable in understanding the properties of general low-dimensional systems [7]. Therefore, much theoretical [8–10] and experimental [1–4, 11–13] effort has been devoted to the investigation of thermal transport properties of CNTs, which is of great importance to both fundamental research and technological applications. Despite much progress in the field, only a few works have been devoted to the effects of structural deformation, which is important and unavoidable in real applications. One of the important recent experimental findings on this subject is that CNTs and boron nitride nanotubes are perfect phonon waveguides with robust thermal transport against severe structural deformations [14]. This indicates an essential distinction between electronic transport and thermal transport in quasi-1D systems, since structural deformations as well as other defects are found to result in a strong scattering of electrons. Motivated by the above experiment [14], we theoretically study thermal transport in CNTs, focusing on the influence of radial strain, to explore the physics underlying the robustness of thermal transport in nanotubes.

Radial compression of the CNT, first observed in 1993 [15], occurs when the CNT makes contact with the substrate or other CNTs [16] and is capable of inducing metal-to-semiconductor or semiconductor-to-metal transitions [17–19]. Until now, electronic transport properties of deformed CNTs have been extensively studied [17–21]; however, understanding of their thermal transport properties is far from satisfactory. Several works on the thermal properties of nanostructures showed that mechanical instability is likely to appear in single-walled CNTs under an axial compression of about 6%, which is believed to induce a decrease in conductance [22, 23]. Such unique properties of single-layer structures make CNTs different from 1D nanowires that have a bulk-like response to axial strain. However, CNTs endure a reversible deformation under quite a high radial strain [18, 24, 25]. It is expected that the thermal behavior of CNTs under radial strain is different from that under axial strain, resulting from different structural responses. However, compared to uniaxial deformation, systematic analysis

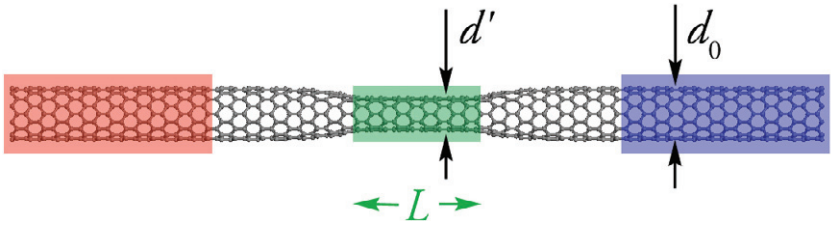

Figure 1. The structure of a radially compressed CNT. The radial strain (η) is defined as $(d_0 - d')/d_0$, where d' is the distance between the fixed opposite atoms and d_0 is the diameter of the ideal CNT without deformation. The confined length (L) is defined as the length of the fixed atom rows. The red and blue areas denote, respectively, the hot and cool reservoirs composed of undeformed CNTs.

of radially deformed CNTs lags behind [26]. A physical picture of the influence of radial deformation on thermal transport properties is crucial for building future CNT-based devices.

In this work, using the nonequilibrium Green's function (NEGF) method, we demonstrate the influence of radial strain on the thermal transport properties of various CNTs with different diameters and chiralities. Quite different from ordinary materials, the thermal conductance of CNTs exhibits a robust linear response to radial strain within the entire elastic range. This behavior generally emerges in nanotubes, independent of diameter and chirality. Our results are consistent with the experiment that shows thermal transport in CNTs intact to structural deformation [14]. Moreover, a detailed analysis of the phonon transmission function reveals that a radial deformation within the elastic range can actually be viewed as a perturbation of the transport of low-frequency phonons, because the seamless cylinder structure is preserved and the C–C bond lengths are changed only slightly. The quasi-ballistic transport of low-frequency phonons leads to the robust thermal transport observed in nanotubes.

2. The model and method

The transport system can be divided into three parts: two semi-infinite pristine CNTs serving as reservoirs and a deformed central part (transport channel), as shown in figure 1. To apply a specified radial strain, two rows of carbon atoms on opposite sides of CNTs are fixed during the structural relaxation. The length of the fixed atom rows is defined as the confined length (L) (see figure 1). The structural relaxation is performed by using the 'General Utility Lattice Program' (GULP) [27], with the Brenner potential [28]. Deformation of the system will delocalize sidewards, inducing a gradually varying deformed tube from the confined region to the pristine reservoirs. For the CNT with a certain confined length L, the larger the radial strain (η), the more extensive the deformation. In all the structural relaxations, the length of the central region is selected long enough to include a complete deformation area from the confined regime to the pristine CNT reservoirs.

Thermal conductance of the deformed system is given by the Landauer formula

$$\sigma(T) = \frac{k_B^2 T}{2\pi\hbar} \int_0^\infty \mathrm{d}x \frac{x^2 \mathrm{e}^x}{(\mathrm{e}^x - 1)^2} \Xi\left(\frac{k_B T}{\hbar} x\right), \tag{1}$$

where $x = \hbar\omega/(k_B T)$ is a dimensionless parameter, $\hbar$ is the reduced Planck constant, ω is the phonon frequency, k_B is the Boltzmann constant and T is the temperature. $\Xi(\omega)$ is the

transmission of the channel, evaluated by the NEGF method [29]:

$$\Xi(\omega) = \mathrm{Tr}(\Gamma_L \mathbf{G}_r \Gamma_R \mathbf{G}_r^{\dagger}), \tag{2}$$

where the spectral density, $\mathbf{\Gamma}_\alpha = \mathrm{i}(\mathbf{\Sigma}_\alpha - \mathbf{\Sigma}_\alpha^{\dagger})$, describes the coupling between the left/right thermal lead ($\alpha = \mathrm{L}$ or R) and the central part (C), with self-energies $\mathbf{\Sigma}_\alpha = \mathbf{D}_{\mathrm{C}\alpha}\mathbf{g}_{\alpha\alpha}\mathbf{D}_{\alpha\mathrm{C}}$. The retarded Green's function of the central part, $\mathbf{G}_r$, is defined as $\mathbf{G}_r = [(\omega + \mathrm{i}\delta)^2\mathbf{M} - \mathbf{D}_{\mathrm{CC}} - \mathbf{\Sigma}_\mathrm{L} - \mathbf{\Sigma}_\mathrm{R}]^{-1}$. Given the diagonal matrix $\mathbf{M}$ with elements corresponding to atomic mass and the dynamical matrix $\mathbf{D}$ of the system, the retarded surface Green's function $\mathbf{g}_{\alpha\alpha} = [(\omega + \mathrm{i}\delta)^2\mathbf{M} - \mathbf{D}_{\alpha\alpha}]^{-1}$ can be derived from Dyson's equation, with δ standing for a small broadening factor for preventing divergence during matrix inversion.

The NEGF method can exactly deal with the thermal transport of the system in which phonon–phonon scattering and electron–phonon scattering are neglected, which is reasonable at a moderate temperature for a sample a few microns long, verified by experiments [3, 4, 11, 12]. Herein, only the heat current mediated by phonons is considered, while the contribution from electrons is neglected [8, 9].

3. Results and discussion

In this section, we systematically investigate the thermal transport behavior of CNTs under radial strain. First, using the (10, 0) CNT as a representative system, we study the effects of interface scattering in radially deformed CNTs. Then we explore the general features of the radial-strain-dependent thermal conductance at different temperatures, and discuss the related physical mechanism. Finally, the size and chirality dependences of thermal conductance are analyzed.

3.1. Interface scattering in radially deformed carbon nanotubes

Figure 2 shows the thermal conductance and phonon transmission function of the perfect and radially deformed (10, 0) CNTs. It can be seen that at low temperatures close to 0 K, thermal conductance is linearly dependent on T (see figure 2(a)), consistent with previous experimental measurements [11, 30]. This is caused by the quantized thermal conductance in units of the quantum thermal conductance $\sigma_0 = (9.456 \times 10^{-13}\,\mathrm{W\,K^{-2}})T$. CNTs have four acoustic phonon modes and thus have thermal conductance of $4\sigma_0$ at low temperatures. As the temperature increases, phonon modes with higher frequencies are excited and contribute to the thermal transport, and consequently thermal conductance increases as shown in figure 2(a).

In the ideal undeformed CNT, phonon transport is ballistic, which is evidenced by the integer phonon transmission function presented in figure 2(b). This is because no structural scattering occurs due to the periodicity of the structure, and other scattering mechanisms, such as electron–phonon scattering and phonon–phonon scattering, are neglected here. Actually, the ballistic thermal conductance in figure 2(a) gives the upper limit of thermal conductance for the pristine (10, 0) CNT. When the radial strain is applied, structural irregularity is introduced and phonons experience scattering when transporting across the deformed regime. Thermal conductance of the CNT decreases when applying radial strain, and the decrease of thermal conductance is very small at low temperatures and gets larger with increasing temperature. As is well known, low-temperature thermal conductance is mainly contributed by low-frequency phonons. Since the transport of most long-wavelength acoustic phonons is insensitive to the

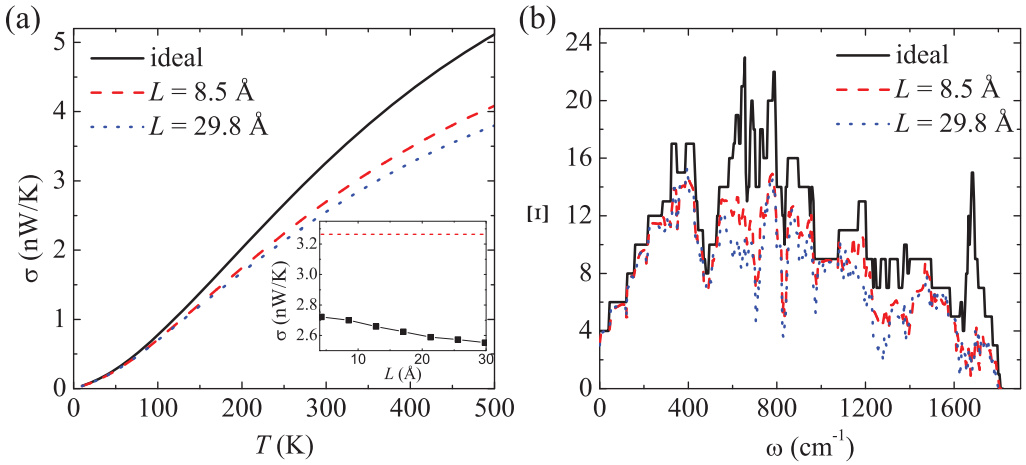

Figure 2. (a) The thermal conductance (σ) versus temperature (T) and (b) the transmission function (Ξ) versus phonon frequency (ω) for the ideal undeformed (10, 0) CNT ($\eta = 0\%$) and two radially deformed (10, 0) CNTs ($\eta = 40\%$) with the confined lengths of $L = 8.5$ and 29.8 Å. The inset in (a) shows the room-temperature thermal conductance versus the confined lengths L for the (10, 0) CNT with a radial strain of $\eta = 40\%$, in comparison with the room-temperature thermal conductance for the ideal undeformed (10, 0) CNT (red broken line).

local deformation, radial strain causes very small scattering in the low-frequency regime, as shown in figure 2(b). The situation is quite different for high-frequency phonons, whose transmission function shows a significant decrease on applying radial strain. Therefore, the frequency-dependent phonon scattering is responsible for the temperature dependence of the thermal conductance decrease caused by radial strain.

It is found that thermal conductance is also dependent on the length L of the confined regime in the transport system. The L-dependent room-temperature ($T = 300$ K) thermal conductance is shown in the inset of figure 2(a) for the (10, 0) CNT with the radial strain of $\eta = 40\%$. Compared with the ideal undeformed (10, 0) CNT, the room-temperature thermal conductance of the deformed tube decreases by about 0.6 nW K^{-1} because of the applied radial strain. Interestingly, the room-temperature thermal conductance decreases only slightly with increasing L and quickly converges to a constant value. In detail, when L increases from 8.5 to 29.8 Å, the room-temperature thermal conductance of the (10, 0) CNT has a very small decrease of 0.15 nW K^{-1} (i.e. only $\sim$4% of the ballistic room-temperature thermal conductance). As L varies, the phonon transmission function shows little change in almost all of the low-frequency regime and most of the high-frequency regime (presented in figure 2(b)). Our results clearly show that thermal conductance is insensitive to the length of the confined regime if the length is not too short, indicating that phonon scattering mainly occurs close to the interface and the coupling between the two interfaces is rather weak. We thus choose $L \sim 8$ Å in the following calculations.

Graphene nanoribbons can be regarded as unzipped CNTs. Our previous work showed that the interface scattering in graphene junctions, composed of graphene nanoribbons with different widths, is basically the main origin of the thermal conductance decrease [31]. It is very interesting to compare the interface scatterings in graphene junctions with those in deformed

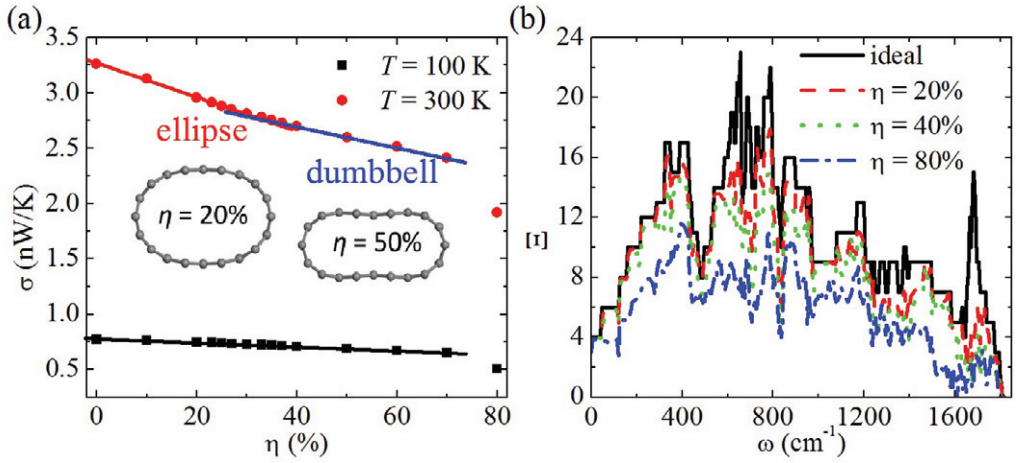

Figure 3. (a) The thermal conductance (σ) of the (10, 0) CNT versus the radial strain (η) at temperatures $T = 100$ and 300 K. The lines are a guide to the eyes. The inset shows the cross-sectional views of the (10, 0) CNT under radial strains of $\eta = 20$ and 50%, which have the shape of an ellipse and a dumbbell, respectively. (b) The transmission function (Ξ) versus phonon frequency (ω) for the (10, 0) CNT under different radial strains: $\eta = 0\%$ (i.e. undeformed), 20%, 40% and 80%.

CNTs. A common feature is that phonon scattering is localized close to the interfacial region and thermal conductance shows little change when the length of the confined region is varied. In contrast, interface scattering has a much smaller influence on low-frequency phonon modes in deformed CNTs than in graphene junctions. Radially deformed CNTs approximately preserve the original bond configuration [19], and only introduce a small mode mismatch between the thermal reservoirs and the transport channel of the transport system. Benefiting from the seamless cylinder structure, CNTs has very high thermal conductivity [1–4]. We find that the superior thermal transport properties are preserved in CNTs under radial deformation. This suggests that CNTs are perfect phonon waveguides, remarkably resistant to severe structural deformations, consistent with the experimental observation of Chang *et al* [14].

3.2. Radial strain-dependent thermal conductance

Now we turn our attention to the effects of different levels of radial strain on the thermal transport properties of CNTs, in order to quantify the dependence of thermal conductance on radial strain. The radial strain-dependent thermal conductance of the (10, 0) CNT is shown in figure 3(a). It can be seen that structural deformation induced by radial strain introduces phonon scattering and thus decreases thermal conductance. The larger the radial strain applied, the lower thermal conductance of the system. In the range of most radial strains, the structural deformation is elastic and a moderate thermal conductance decrease is observed. In contrast, thermal conductance has a sharp drop at very high strain ($\sim 80\%$ in the (10, 0) CNT). This sudden decrease is caused by the inelastic deformation, which is due to the formation of sp^3 bonds between the opposite walls of the CNT, changing the bonding configuration of the system. When sp^3 bonds appear, the mechanical properties of the system change significantly, and a

super-hard state appears [32, 33], leading to serious phonon scattering at the junctions between the deformed part and the reservoirs. This is evidenced by the phonon transmission function shown in figure 3(b): the inelastic deformation ($\eta = 80\%$) obviously decreases transmission function not only in the high-frequency regime but also in the low-frequency regime, and thus significantly reduces thermal conductance.

More interestingly, the radial strain-dependent thermal conductance of the deformed CNT (presented in figure 3(a)) shows some unique characteristics that are very unusual for most materials. At low temperatures (such as $T = 100$ K), the thermal conductance is linearly dependent on radial strain. The behavior seems to be trivial at first glance because the linear response is general in a number of physical systems where a weak external perturbation is added. Unexpectedly, the linear dependence is preserved in an extremely wide range even when the radial strain increases to 70%. At low temperatures, only low-frequency phonon modes are populated, whose transport is slightly influenced by radial deformation. As long as the structural deformation is elastic (i.e. the bond configuration of the transport channel is kept), low-frequency phonon modes in CNTs under radial strain are less affected by the deformation and thus the induced interface scattering is small. Note that elastic deformation occurs even under a large radial strain up to 70%, and in this case the strain applied can be considered as a perturbation of the low-temperature thermal transport. This is the physical origin of the robust linear response found in the radially deformed CNTs.

As the temperature increases, new features appear in the strain-dependent thermal conductance. In contrast to the simple linear dependence at low temperatures, the room-temperature thermal conductance versus radial strain (shown in figure 3(a)) behaves differently in the low-strain and high-strain regimes. The linear dependence is kept at the two regimes separately; moreover, the change in thermal conductance is faster at low strain than at high strain. The same phenomenon is observed at higher temperatures (data not shown). A detailed analysis shows that the conductance transition corresponds to a structural transition: an elliptical cross section in the low-strain regime and a dumbbell-shaped cross section in the high-strain regime, shown in the inset of figure 3(a). The structural transition (at $\eta \sim 30\%$ for the (10, 0) CNT) gives rise to different linear dependences of the high-temperature thermal conductance on radial strain.

3.3. Effects of tube diameter and chirality

Finally, we discuss the effects of tube diameter and chirality on the thermal transport in radially deformed CNTs. Figures 4(a) and (b) show the thermal conductance of various CNTs with different diameters and chiralities as a function of the applied radial strain at $T = 100$ and 300 K. Similar to that observed in the (10, 0) CNT, the low-temperature thermal conductance is linearly dependent on the radial strain in all of the elastic regime, and the high-temperature thermal conductance shows different linear dependences in the low-strain and high-strain regimes due to an ellipse–dumbbell structural transition. In addition, thermal conductance has a sharp decrease when the deformation goes into the inelastic regime (data not shown). Our results show that these features are general in all CNTs, independent of their diameter and chirality.

We further compare the slope of the thermal conductance versus radial strain lines for elastically deformed CNTs, as shown in figures 4(c) and (d). The slope is much more negative at higher temperature due to the strong phonon scattering at high frequencies. It should be noted that two lines are used to fit the thermal conductance versus radial strain curve at $T = 300$ K as

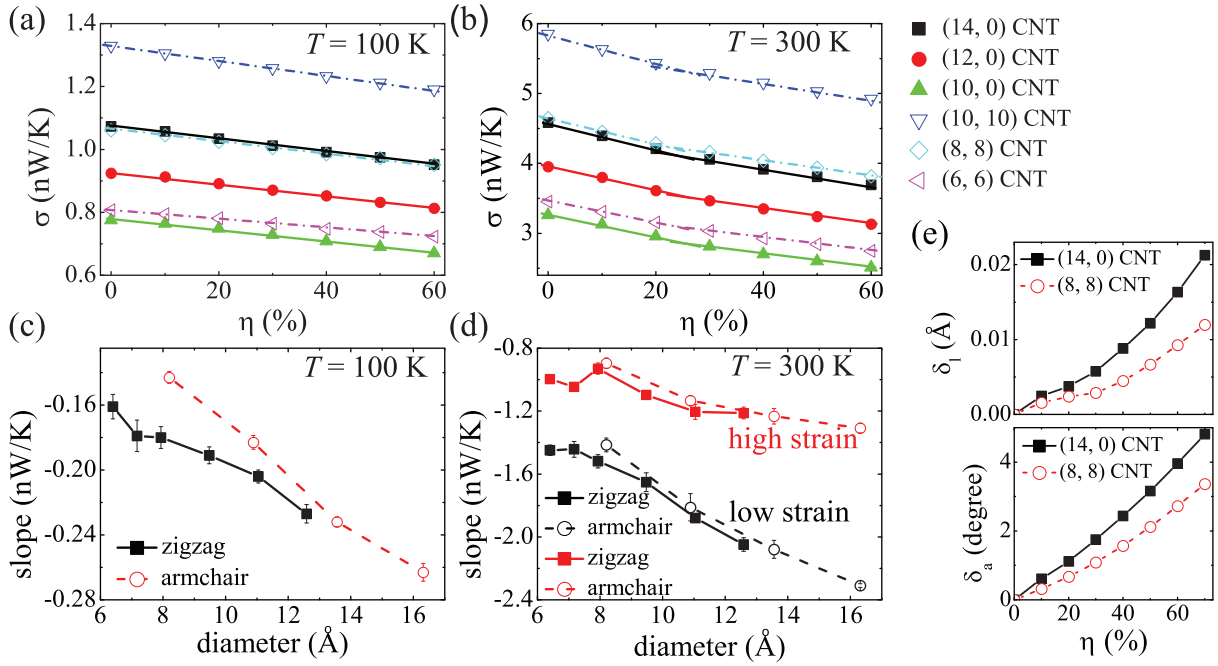

Figure 4. Thermal conductance (σ) of CNTs at temperatures (a) $T = 100$ K and (b) $T = 300$ K versus the applied radial strain (η). The slopes of the curves in (a) and (b) are given as a function of the diameter of zigzag and armchair CNTs at temperatures (c) $T = 100$ K and (d) $T = 300$ K. Each curve in (b) is described by two lines and therefore two slopes are given in (d) for the low-strain and high-strain regimes separately. (e) The maximum deviations (δ_l and δ_a) in the bond lengths and bond angles of the (14, 0) CNT and the (8, 8) CNT versus radial strain.

shown in figure 4(b); thus two slopes are given in figure 4(d) for the low-strain and high-strain regimes separately. It is clearly seen that the thermal conductance decreases faster in the low-strain regime than in the high-strain regime. On analyzing the phonon transmission as a function of radial strain, we find that the transmission of high-frequency phonons decreases faster in the low-strain regime, but such a decrease slows down as the strain increases further. These high-frequency phonons contribute significantly to the high-temperature thermal conductance and result in the difference of the slopes at high temperatures.

Moreover, the slope obtained shows interesting diameter and chirality dependences (see figures 4(c) and (d)). CNTs of larger diameters have an obviously faster decrease of thermal conductance. The underlying reason is that larger CNTs have more phonon transport channels and can be more easily distorted; thus applying the same radial strain causes a larger absolute decrease in the phonon transmission function. In contrast, the chirality effect on the slope is small but is still not negligible. The slopes of zigzag CNTs are slightly more negative than those of armchair CNTs. Such an anisotropy is not straightforward, considering that thermal transport is isotropic in pristine CNTs [34]. To explain the anisotropy, we select two CNTs of similar diameters: the zigzag (14, 0) CNT and the armchair (8, 8) CNT. The maximum deviations in the bond lengths and bond angles, corresponding to the distortion degree of the system in comparison with the undeformed one, are given as functions of radial strain in figure 4(e). It can

be seen that the zigzag CNT has a larger bond distortion than the armchair CNT under the same strain, resulting in larger phonon scattering. This may directly give rise to the small anisotropy of thermal conductance observed in radially deformed CNTs.

4. Conclusions

In conclusion, the thermal transport in radially deformed CNTs shows rich and interesting properties. Radial strain introduces structural irregularity in CNTs, thus causing phonon scattering, which mainly occurs near the interface. In contrast to the interface scattering in other systems (such as graphene junctions [31]), phonons of low frequencies experience little scattering and the low-temperature thermal conductance has negligible decrease. Radial strain in CNTs can be viewed as a perturbation of the transport of low-frequency phonons; therefore a robust linear response of thermal conductance to radial strain appears in the entire elastic range at low temperatures. In contrast, radial strain causes significant scattering of high-frequency phonons and thermal conductance shows an obvious decrease at high temperatures. When high-frequency phonons are significantly involved in thermal transport, the thermal conductance versus radial strain curve shows different linear dependences in the low-strain and high-strain regimes because of an ellipse–dumbbell structural transition. In addition, thermal conductance decreases faster in CNTs of larger diameters and the slope of a thermal conductance versus radial strain line shows a weak chirality dependence: zigzag CNTs give a slightly more negative slope than armchair CNTs. In the case of a very high radial strain, the structural deformation becomes inelastic and thermal conductance significantly decreases due to the severe change in mechanical properties.

This paper presents a quantitative description of the radial strain-dependent thermal conductance for various CNTs and clearly reveals general features of the thermal transport in CNTs under radial strain. In particular, CNTs are shown to be perfect phonon waveguides, consistent with the experimental observation [14]. These findings will provide guidance on future applications of CNTs in thermal management.

Acknowledgments

This work was supported by the Ministry of Science and Technology of China (grant numbers 2011CB921901 and 2011CB606405) and the National Natural Science Foundation of China (grant no. 11074139). YX acknowledges support from the Alexander von Humboldt Foundation.

References

[1] Kim P, Shi L, Majumdar A and McEuen P L 2001 *Phys. Rev. Lett.* **87** 215502
[2] Pop E, Mann D, Wang Q, Goodson K and Dai H 2006 *Nano Lett.* **6** 96
[3] Yu C, Shi L, Yao Z, Li D and Majumdar A 2005 *Nano Lett.* **5** 1842
[4] Fujii M, Zhang X, Xie H, Ago H, Takahashi K, Ikuta T, Abe H and Shimizu T 2005 *Phys. Rev. Lett.* **95** 065502
[5] Lin W, Zhang R W, Moon K S and Wong C P 2010 *Carbon* **48** 107
[6] Kordás K, Tóth G, Moilanen P, Kumpumäki M, Vähäkangas J, Uusimäki A, Vajtai R and Ajayan P M 2007 *Appl. Phys. Lett.* **90** 123105

[7] Cahill D G, Ford W K, Goodson K E, Mahan G D, Majumdar A, Maris H J, Merlin R and Phillpot S R 2003 *J. Appl. Phys.* **93** 793
[8] Yamamoto T, Watanabe S and Watanabe K 2004 *Phys. Rev. Lett.* **92** 075502
[9] Mingo N and Broido D A 2005 *Phys. Rev. Lett.* **95** 096105
[10] Wang J and Wang J-S 2006 *Appl. Phys. Lett.* **88** 111909
Donadio D and Galli G 2007 *Phys. Rev. Lett.* **99** 255502
Wu G and Li B 2007 *Phys. Rev.* B **76** 085424
Lü J T and Wang J-S 2008 *Phys. Rev.* B **78** 235436
Stoltz G, Mingo N and Mauri F 2009 *Phys. Rev.* B **80** 113408
Lindsay L, Broido D A and Mingo N 2010 *Phys. Rev.* B **82** 161402
Ni X, Leek M L, Wang J-S, Feng Y P and Li B 2011 *Phys. Rev.* B **83** 045408
Dubi Y and Ventra M D 2011 *Rev. Mod. Phys.* **83** 131
[11] Hone J, Whitney M, Piskoti C and Zettl A 1999 *Phys. Rev.* B **59** 2514
[12] Pop E, Mann D, Cao J, Wang Q, Goodson K and Dai H 2005 *Phys. Rev. Lett.* **95** 155505
[13] Choi T-Y, Poulikakos D, Tharian J and Sennhauser U 2006 *Nano Lett.* **6** 1589
Chang C W, Okawa D, Garcia H, Majumdar A and Zettl A 2008 *Phys. Rev. Lett.* **101** 075903
Kunadian I, Andrews R, MenguÇ M P and Qian D 2009 *Carbon* **47** 589
Baloch K H, Voskanian N and Cumings J 2010 *Appl. Phys. Lett.* **97** 063105
[14] Chang C W, Okawa D, Garcia H, Majumdar A and Zettl A 2007 *Phys. Rev. Lett.* **99** 045901
[15] Ruoff R S, Tersoff J, Lorents D C, Subramoney S and Chan B 1993 *Nature* **364** 514
[16] Hertel T, Walkup R E and Avouris P 1998 *Phys. Rev.* B **58** 13870
[17] Tombler T W, Zhou C, Alexseyev L, Kong J, Dai H, Liu L, Jayanthi C S, Tang M and Wu S-Y 2000 *Nature* **405** 769
[18] Lu J Q, Wu J, Duan W H, Liu F, Zhu B F and Gu B-L 2003 *Phys. Rev. Lett.* **90** 156601
Lu J Q, Wu J, Duan W H and Gu B-L 2004 *Appl. Phys. Lett.* **84** 4203
[19] Gülseren O, Yildirim T, Ciraci S and Kılıç Ç 2002 *Phys. Rev.* B **65** 155410
[20] Yang L and Han J 2000 *Phys. Rev. Lett.* **85** 154
[21] Minot E D, Yaish Y, Sazonova V, Park J-Y, Brink M and McEuen P L 2003 *Phys. Rev. Lett.* **90** 156401
[22] Xu Z and Buehler M J 2009 *Nanotechnology* **20** 185701
[23] Li X, Maute K, Dunn M L and Yang R 2010 *Phys. Rev.* B **81** 245318
[24] Chesnokov S A, Nalimova V A, Rinzler A G, Smalley R E and Fischer J E 1999 *Phys. Rev. Lett.* **82** 343
[25] Tang J, Qin L-C, Sasaki T, Yudasaka M, Matsushita A and Iijima S 2000 *Phys. Rev. Lett.* **85** 1887
[26] Zhong W-R, Zhang M-P, Zheng D-Q and Ai B-Q 2011 *J. Appl. Phys.* **109** 074317
[27] Gale J D 1997 *J. Chem. Soc. Faraday Trans.* **93** 629
[28] Brenner D W 1990 *Phys. Rev.* B **42** 9458
[29] Yamamoto T and Watanabe K 2006 *Phys. Rev. Lett.* **96** 255503
Wang J-S, Wang J and Zeng N 2006 *Phys. Rev.* B **74** 033408
Xu Y, Wang J-S, Duan W H, Gu B-L and Li B 2008 *Phys. Rev.* B **78** 224303
[30] Schwab K, Henriksen E A, Worlock J M and Roukes M L 2000 *Nature* **404** 974
[31] Xu Y, Chen X, Wang J-S, Gu B-L and Duan W H 2010 *Phys. Rev.* B **81** 195425
[32] Shen W, Jiang B, Han B S and Xie S-S 2000 *Phys. Rev. Lett.* **84** 3634
[33] Zhu C Z, Guo W, Yu T X and Woo C H 2005 *Nanotechnology* **16** 1035
[34] Xu Y, Chen X, Gu B-L and Duan W H 2009 *Appl. Phys. Lett.* **95** 233116